Biochemical and Biophysical Research Communications 451 (2014) 485–490

Contents lists available at ScienceDirect

Biochemical and Biophysical Research Communications

journal homepage: www.elsevier.com/locate/ybbrc

Identification of borrelidin binding site on threonyl-tRNA synthetase

Ming Li [a,1], Ji Zhang [a,1], Chongxi Liu [a], Baozhu Fang [a], Xiangjing Wang [a,*], Wensheng Xiang [a,b,*]

[a] Key Laboratory of Agriculture Biological Functional Gene of Heilongjiang Provincial Education Committee, Northeast Agricultural University, No. 59 Mucai Street, Xiangfang District, Harbin 150030, PR China
[b] State Key Laboratory for Biology of Plant Diseases and Insect Pests, Institute of Plant Protection, Chinese Academy of Agricultural Sciences, Beijing 100193, PR China

ARTICLE INFO

Article history:
Received 4 July 2014
Available online 13 August 2014

Keywords:
Borrelidin
Threonyl-tRNA synthetase
Molecular docking
Site-directed mutagenesis
Stopped-flow fluorimetry

ABSTRACT

Borrelidin exhibits a wide spectrum of biological activities and has been considered as a non-competitive inhibitor of threonyl-tRNA synthetase (ThrRS). However, the detailed mechanisms of borrelidin against ThrRS, especially borrelidin binding site on ThrRS, are still unclear, which limits the development of novel borrelidin derivatives and rational design of structure-based ThrRS inhibitors. In this study, the binding site of borrelidin on *Escherichia coli* ThrRS was predicted by molecular docking. To validate our speculations, the ThrRS mutants of *E. coli* (P424K, E458Δ, and G459Δ) were constructed and their sensitivity to borrelidin was compared to that of the wild-type ThrRS by enzyme kinetics and stopped-flow fluorescence analysis. The docking results showed that borrelidin binds the pocket outside but adjacent to the active site of ThrRS, consisting of residue Y313, R363, R375, P424, E458, G459, and K465. Site-directed mutagenesis results showed that sensitivities of P424K, E458Δ, and G459Δ ThrRSs to borrelidin were reduced markedly. All the results showed that residue Y313, P424, E458, and G459 play vital roles in the binding of borrelidin to ThrRS. It indicated that borrelidin may induce the cleft closure, which blocks the release of Thr-AMP and PPi, to inhibit activity of ThrRS rather than inhibit the binding of ATP and threonine. This study provides new insight into inhibitory mechanisms of borrelidin against ThrRS.

1. Introduction

Aminoacyl-tRNA synthetases (aaRSs), the central enzymes in protein translation, catalyze the covalent attachment of correct amino acids to their cognate tRNAs, yielding the aminoacyl tRNAs (aa-tRNA or charged tRNA) used for protein synthesis. Despite the fact that all aaRSs share the same reaction mechanism and universally distribute in cellular organisms, the high level of phylogenetic divergence between prokaryotic and eukaryotic enzymes implies the potent development of selective inhibitors to discriminate the aaRSs between pathogen and host. Once one of these enzymes is inhibited, aminoacyl-tRNAs biosynthesis can be halted, which in turn stalls elongation of growing polypeptide chains [1]. Due to the pivotal role in protein synthesis, aaRSs have been considered as some of the most promising targets for antibiotics development in pathogenic species. Compounds that inhibit aaRSs have been successfully exploited, with at least one antibacterial drug, mupirocin A, currently the world's leading topical antibiotic for the topical treatment of methicillin-resistant *Staphylococcus aureus* infections, which acts through the inhibition of the isoleucyl-tRNA synthetase (IleRS) of gram-positive bacteria [2]. Other natural product aaRS inhibitors consist of reveromycin A (targets IleRS), borrelidin (targets ThrRS), indolmycin (targets TrpRS), ochratoxin (targets PheRS), cispentacin (targets ProRS), and granaticin (targets LeuRS) [1,3]. Besides, some synthetic aaRS inhibitors are also developed as variants of the natural substrate or as non-hydrolyzable aa-AMP mimics [4], most of which act through competitive binding to the aaRSs. Although the aa-AMP mimics demonstrated low nanomolar binding affinities against their corresponding aaRSs, the lack of selectivity and poor bacterial cell permeability are the most prominent problems for this new potential class of antibiotics.

Borrelidin, an 18-membered macrolide polyketide produced by several actinomycete bacteria of the *Streptomyces* spp, exhibits a wide spectrum of biological activities, such as antibacterial activity [5], antiviral activity [6], anti-angiogenesis [7,8], antimalarial activity [9], and insecticidal and herbicidal activities [10]. Some of these activities are associated with the inhibition of threonyl-tRNA synthetase (ThrRS); however, in contrast to most of the aaRS inhibitors, borrelidin is an allosteric inhibitor of ThrRS that can

* Corresponding authors. Address: Key Laboratory of Agriculture Biological Functional Gene of Heilongjiang Provincial Education Committee, Northeast Agricultural University, No. 59 Mucai Street, Xiangfang District, Harbin 150030, PR China (W. Xiang). Fax: +86 0451 55190413.
E-mail addresses: wangneau2013@163.com (X. Wang), xiangwensheng@neau.edu.cn (W. Xiang).
[1] Ming Li and Ji Zhang contributed equally to this work.

http://dx.doi.org/10.1016/j.bbrc.2014.07.100
0006-291X/

non-competitively and tightly bind to ThrRS [11]. The remarkable bioactivities have prompted the development of synthetic derivatives of borrelidin for use as pharmaceutically important lead candidates. Screening of random *Escherichia coli* ThrRS borrelidin-resistant mutants suggested that borrelidin inhibits ThrRS by binding to a unique hydrophobic patch proximal to a divalent Zn^{2+} binding site, leading to impair catalytic conformational changes necessary for threonine and ATP binding [12]. However the absence of a co-crystal structure of ThrRS in complex with borrelidin precludes an exact description of the nature of the binding interaction.

In order to further understand the antibacterial mechanism of borrelidin, this compound was docked into ThrRS. Surprisingly, the hydrophobic patch, which was previously considered as the binding site of borrelidin, was found too small to accommodate borrelidin. In this study, a suitable binding mode of borrelidin into ThrRS was predicted, and the key amino acid residues involving the binding of borrelidin were identified by molecular docking and further confirmed by mutagenesis and enzyme kinetic assay.

2. Materials and methods

2.1. Borrelidin and ATP docking to E. coli ThrRS

Crystal structure of the *E. coli* threonyl-tRNA synthetase–$tRNA^{Thr}$ complex was obtained from PDB (PDB ID: 1QF6). Borrelidin and ATP were taken from the PubChem database (Compound ID: 6436801 and 5957, respectively). Considering induced fit of ThrRS by borrelidin binding, flexible docking of borrelidin to *E. coli* ThrRS was performed using the AutoDock Vina program [13], and the ligands and receptor molecules were prepared using AutoDock Tools 1.5.6 [14]. A grid map around cluster A reported by Ruan et al. [12], was defined with a size of 30 Å × 30 Å × 30 Å, a grid center of 25.835 × 73.1 × 52.303, and spacing of 0.375 Å between the grid points. Thr307, His309, Cys334, Pro335, Leu489 and L493, which consists of cluster A, were selected as flexible side-chain residues. Maximum number of binding modes to generate and exhaustiveness of the global search were 30 and 30, respectively. For ATP, rigid docking was performed using AutoDock Vina, and the grid center co-ordinate was adjusted to the ThrRS active site. The docking conformation with the lowest binding free energy was used for further analysis by AutoDock Tools 1.5.6.

2.2. Sequence alignments of E. coli ThrRS and other ThrRSs species

The sequences of ThrRSs from *E. coli*, *Phytophthora sojae* [15], *Sulfolobus solfataricus*, *Methanocaldococcus jannaschii*, and *Archaeoglobus fulgidus* [12] were aligned using the Clustalx 1.8 software [16].

2.3. Site-directed mutagenesis

The gene *ThrRS* was amplified from genomic DNA of *E. coli* K-12 using a pair of primers P1 and P2 (Table 1). Amplification reaction was conducted by standard procedure with an annealing temperature of 52 °C. The PCR products were digested with *Bam*HI and *Hin*dIII and inserted into pET-21b (+) to give the expression plasmid pET-21b-*ThrRS*. Mutagenesis of ThrRS was performed using overlapping PCR [17]. The plasmid pET-21b-*ThrRS* was used as template, and the primers listed in Table 1 were used for site-directed mutagenesis to yield the desired mutants. Then, the obtained mutants were inserted into pET-21b (+) to generate plasmid pET-21b–P424K, pET-21b–E458Δ, and pET-21b–G459Δ, respectively.

Table 1
Primers used for PCR amplification of *ThrRS* and constructing the mutants.

Name of primer	Sequence[a]
Forward primer (P1)	5′-GGAAGATCTATGCCTGTTATAACTCTTCC-3′
Backward primer (P2)	5′-CCCAAGCTTTTCCTCCAATTGTTTAAGAC-3′
Forward primer for P424K	5′-CACTCGTAAAGAAAAACGTATTGGCAG-3′
Backward primer for P424K	5′-CGTTTTTCTTTACGAGTGGAGAGTTTG-3′
Forward primer for E458Δ	5′-ACTGGGTGGCGCTTTCTACGGTCCGAA-3′
Backward primer for E458Δ	5′-TAGAAAGCGCCACCCAGTTGATATTCA-3′
Forward primer for G459Δ	5′-GGGTGAAGCTTTCTACGGTCCGAAAAT-3′
Backward primer for G459Δ	5′-CCGTAGAAAGCTTCACCCAGTTGATAT-3′

[a] Underlined sequence for restriction enzyme recognition sites.

2.4. Expression and purification of recombinant enzymes

After sequence confirmation, the constructed plasmid was transformed into *E. coli* BL21 (DE3). After the cells harboring recombinant plasmid were grown in LB medium at 37 °C to an absorbance at OD_{600} of about 0.6 and induced by the addition of 0.5 mM isopropyl-β-D-thiogalactoside (IPTG), the cells were incubated at 16 °C for an additional 20 h. The cells were harvested by centrifugation at 6000×*g* for 10 min at 4 °C, washed with 25 ml of 50 mM Tris–HCl buffer (pH 7.4), and then resuspended in 5 mL of the same buffer. The obtained cell suspension was sonicated and the supernatant was collected by centrifugation (12,000×*g*, 20 min) at 4 °C. His-tagged ThrRS fusion proteins were purified by Ni^{2+} affinity chromatography (Invitrogen) according to the instructions of the manufacturer. The proteins were eluted by the use of a series of elution buffers of imidazole (10, 50, 100, and 150 mM) in the above Tris–HCl buffer. The pure fractions were dialyzed with a storage buffer (50 mM Tris–HCl buffer, pH 7.4) at 4 °C. The purity of the protein was ascertained by sodium monododecyl sulfate (SDS)–polyacrylamide gel electrophoresis (PAGE). Protein concentration was determined by the method of Lowry et al. [18]. The recombinant enzymes were stored at −80 °C prior to use in experiments.

2.5. Circular dichroism

CD measurements were performed with a MOS-450 spectrometer from BioLogic (BioLogic Science Instruments, Claix, France) using a 0.1 mm quartz cell. Acquisition duration was 5 s, with a slit of 2 nm. The readings of the blanks, which included the appropriate solvents, were subtracted from the readings of the sample solutions. CD spectra of protein were recorded in the range of 190–250 nm at 25 °C with 1 nm step size. The protein sample concentration was 0.5 mg/mL. The contents of different secondary structures of protein were analyzed by the online SELCON3 program [19,20].

2.6. Borrelidin inhibition of E. coli ThrRS at the step of threonine activation in vitro

The borrelidin inhibition of *E. coli* ThrRS and its mutants at the step of threonine activation was measured by the method described previously [15]. For determining the steady state kinetic constants K_m and k_{cat}, the enzymes were diluted to obtain linear initial velocities. K_m and k_{cat} were calculated in KaleidaGraph 3.0 using a Michaelis–Menten equation fit. The initial velocities obtained were plotted against borrelidin concentration to obtain IC_{50} values. The apparent inhibition constant $K_i^{(app)}$ values were calculated on the basis of the simplified equation ($K_i^{(app)} = IC_{50} - [E]/2$, where $[E]$ represents the ThrRS concentration used in the experiment) derived for non-competitive tight binding inhibition [21].

2.7. Pre-steady state analysis

Stopped-flow fluorescence was performed using a SFM-300 mixing apparatus connected to a MOS-450 spectrometer (BioLogic, Inc.) under controlled temperature. The reactions contained 20 mM phosphate-buffered saline, pH 7.4, 150 mM KCl, 15 mM $MgCl_2$, 1 μM ThrRS or mutants, and 10 μM borrelidin. The apparent first-order rate constants (K_{app}) were measured by rapidly mixing enzyme with borrelidin at 30 °C.

3. Results

3.1. Borrelidin or ATP docking to wild-type E. coli ThrRS

Borrelidin and ATP were docked to ThrRS using AutoDock Vina, respectively. The docking conformations of borrelidin and ATP with the lowest binding free energy were generated on the ThrRS using AutoDock Tools 1.5.6. Since cluster A was predicted as borrelidin bind pocket previously [12], the center of the search box was defined from the center of mass of cluster A. Surprisingly, for all 20 binding modes generated, the cluster A is not large enough to accommodate borrelidin. Instead, borrelidin binds adjacent to the pocket of ATP binding as shown in Fig. 1A. The docking result in Fig. 1A demonstrated different binding site of borrelidin and ATP on ThrRS, since borrelidin was not overlapped by ATP, implying that borrelidin and ATP could simultaneously bind to ThrRS to form a ThrRS–ATP–borrelidin complex. Additionally, the docking results in Fig. 1B showed that all the amino acid residues associated with borrelidin binding were outside but adjacent to the active site, indicating that borrelidin is a noncompetitive inhibitor of *E. coli* ThrRS with respect to threonine and ATP, which is consistent with previous reports [22]. It should be noted that the binding free energy of borrelidin (−9.1 kcal/mol) was higher than that of ATP (−9.6 kcal/mol), suggesting that the binding of ATP is easier than that of borrelidin. It means that ATP binds to ThrRS previous to borrelidin, and ATP locates deeper than borrelidin in the active pocket of ThrRS. Therefore, we speculated that borrelidin can induce the cleft closure to block the release of Thr-AMP and PPi, rather than inhibits the binding of ATP and threonine. Additionally, the docking results (Fig. 2A) showed that the residues within 3 Å of borrelidin were Y313, R363, R375, P424, E458, G459, and K465, implying the important roles of these residues in the binding of borrelidin to ThrRS. As shown in Fig. 2B, the main residues consisted of cluster A (Thr307, His309, Cys334, Pro335, and Leu489) reported by Ruan [12] were the residues within 10 Å of borrelidin.

In an attempt to further identify the key residues involving borrelidin binding, the amino acid sequences of ThrRSs from *E. coli*, Borrelidin-resistant species (*M. jannaschii* and *A. fulgidus*), and Borrelidin-susceptible species (*S. solfataricus* and *P. sojae*) were aligned, since none crystal structures of *M. jannaschii*, *A. fulgidus*, *S. solfataricus* and *P. sojae* were available. The results demonstrated that residue R363, R375, and K465 are highly conserved in all the ThrRSs, whereas other residues corresponding to Y313, P424, E458, and G459 in *E. coli* ThrRS are variable. Interestingly, these four amino acids are conserved in the Borrelidin-susceptible species *S. solfataricus* and *P. sojae* but variable in Borrelidin-resistant species *M. jannaschii* and *A. fulgidus* (Fig. 3). Since *M. jannaschii*, *A. fulgidus*, and *S. solfataricus* are archaea, but their ThrRSs have different sensitivities to borrelidin. It seems that different sensitivities to borrelidin are not relative to their species but the four different amino residues. Thus, Y313, P424, E458, and G459 may be the more important residues involving the binding of borrelidin, and any change of these residues may affect the sensitivity of ThrRS to Borrelidin.

3.2. Site-directed mutagenesis and kinetic analysis

Since Y313 has been identified as a key residue for borrelidin binding [12], the roles of P424, E458, and G459 in the binding of borrelidin were investigated by site-directed mutagenesis. The corresponding amino acids of E458 and G459 are absent in the borrelidin-resistant ThrRS, two mutants with the deletion of E458 and G459 were then constructed respectively. As shown in Table 2, the deletion of E458 or G459 in *E. coli* ThrRS did not affect enzyme

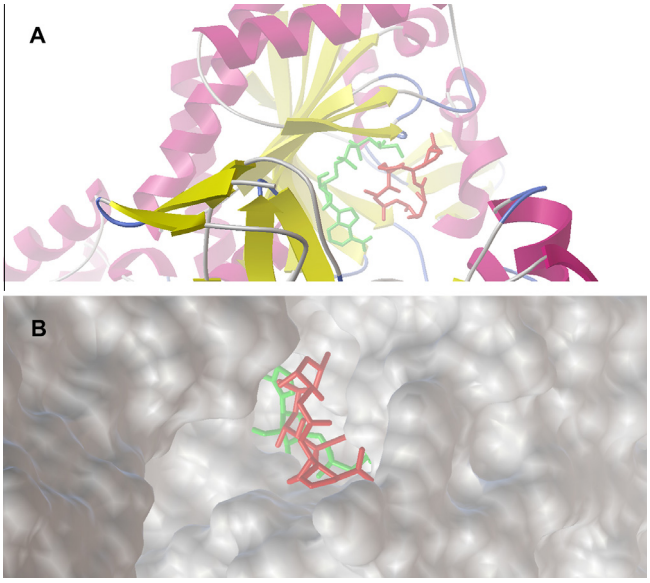

Fig. 1. Detailed stereo view of borrelidin and ATP in ThrRS. Borrelidin is shown in red, and ATP is shown in green. Predicted binding mode of borrelidin docked with ThrRS on molecular surface. (A) Borrelidin was not overlapped by ATP. (B) Borrelidin was outside the pocket of ATP. (For interpretation of the references to color in this figure legend, the reader is referred to the web version of this article.)

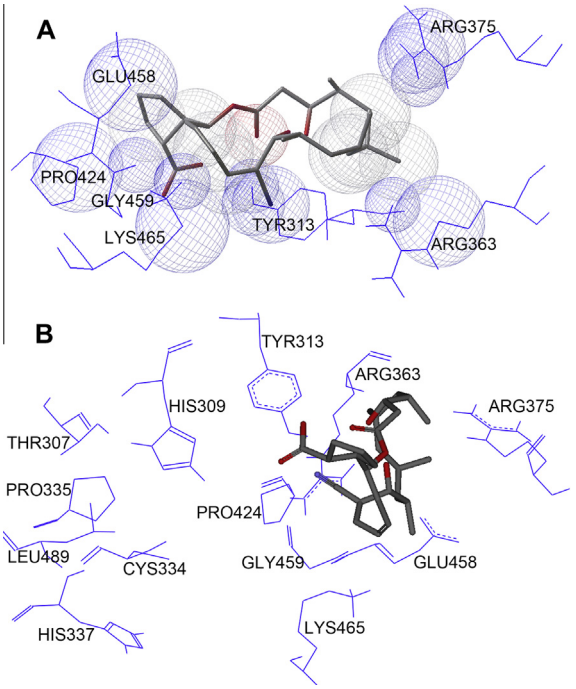

Fig. 2. The interaction between borrelidin and ThrRS. The residues within 3 Å (A) and 10 Å (B) of borrelidin were represented using line structures and the borrelidin structure was represented using stick structures.

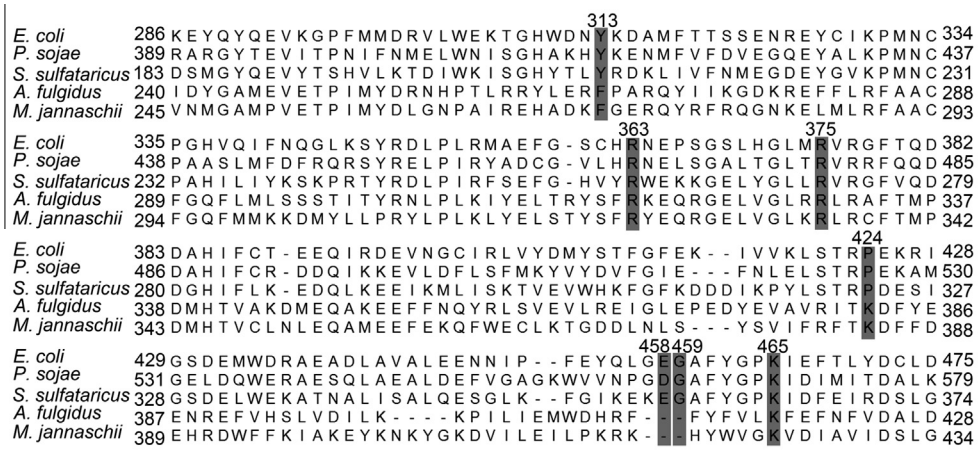

Fig. 3. Protein sequence alignment of *E. coli* ThrRS with Borrelidin-resistant species ThrRSs and Borrelidin-susceptible species ThrRS. The gray region indicates the residues studied. The strictly conserved residues are residue R363, R375, and K465 in *E. coli* ThrRS. The ThrRSs of *M. jannaschii* and *A. fulgidus* exhibit a variable relationship with site 313, 424, 458, and 459 of the *E. coli* ThrRS. The ThrRS of *P. sojae* and *S. solfataricus* are conserved at these sites with respect to the *E. coli* ThrRS.

Table 2
Steady-state kinetic constants of wild-type *E. coli* ThrRS and mutants.

Source of ThrRS	K_m (Thr) [μM]	k_{cat} [s^{-1}]	$K_i^{(app)}$ [nM]	K_{app} [s^{-1}]
E. coli	105 ± 5	35 ± 2.3	3.4 ± 0.2	69 ± 3
P424K	108 ± 5	30 ± 2.3	65.12 ± 5.2	5.1 ± 0.1
E458Δ	104 ± 5	34 ± 2.5	19.1 ± 1.8	8.4 ± 0.2
G459Δ	101 ± 5	28 ± 2.3	111.4 ± 6.6	2.7 ± 0.06

activity, but significantly increased the $K_i^{(app)}$ value approximately 5.3 and 30.1-fold, respectively. The same phenomenon was also observed when P424 in *E. coli* ThrRS was substituted by the counterpart amino acid Lys in the Borrelidin-resistant ThrRS.

Furthermore, the stopped-flow fluorescence studies showed that borrelidin with a concentration of 10 μM can greatly quench the intrinsic fluorescence of wild-type (WT) of ThrRS, but has limited effect on quenching of the intrinsic fluorescence of P424K, E458Δ, and G459Δ (Fig. 4A). To elucidate the function of residue P424, E458, and G459 upon borrelidin binding reaction, the apparent first-order rate constants for borrelidin were determined through stopped flow fluorescence experiments. As listed in Table 2, P424K, E458Δ, and G459Δ ThrRSs exhibit decreased apparent rate constants compared to WT ThrRS, implying that the change of these amino acids can decrease the affinity of borrelidin to ThrRS. On the other hand, the WT, P424K, E458Δ, and G459Δ ThrRSs demonstrated similar CD spectra (Fig. 4B). Comparison of the content of secondary structures (α-helix and β-sheet) in WT ThrRS with those in the mutant ThrRS suggested that the change of P424, E458, or G459 has no effect on the structure of *E. coli* ThrRS. Therefore, we speculated that the decreased affinity of borrelidin to P424K, E458Δ, and G459Δ ThrRSs may be caused by the lower interactions between ThrRS and borrelidin rather than the structural change of ThrRS.

4. Discussion

Aminoacyl-tRNA synthetases are central enzymes in protein translation, providing the charged tRNAs needed for appropriate construction of peptide chains. These enzymes have long been pursued as drug targets in bacteria, fungi, and eukaryotic parasites. In recent years, many inhibitors targeting on the synthetic and editing active sites of aminoacyl-tRNA synthetases are being developed as antibacterials, antifungals and anti-parasitic drugs [23–27]. For example, Mupirocin, an inhibitor targeting on the synthetic active site of IleRS, has been approved by the US Food and Drug Administration for the treatment of bacterial skin infections [28]; AN2690,

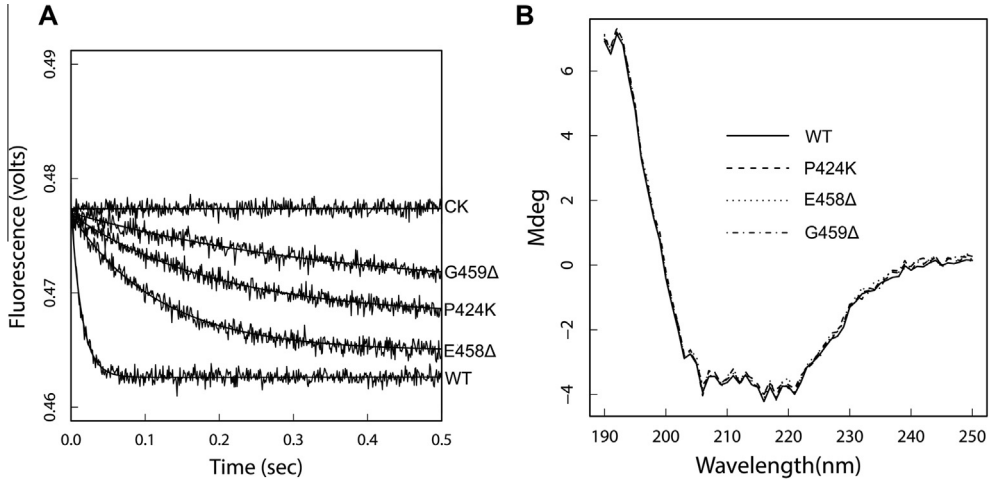

Fig. 4. (A) Intrinsic fluorescence of WT and mutated ThrRSs in the presence of borrelidin. The final concentration of borrelidin is 10 μM, and CK is the curve of enzyme without Borrelidin. (B) Circular dichroism of WT and mutated ThrRSs. Line style of the curve for WT, P424K, E458Δ, and G459Δ ThrRS are solid, dash, dot, and dash dot, respectively.

an inhibitor targeting on the editing active site of LeuRS, is currently in Phase 3 clinical trials for treating onychomycosis [29]. Notably, most of the inhibitors including mupirocin and AN2690 are competitive inhibitors. In contrast to the known aaRS inhibitors, borrelidin is an allosteric inhibitor of ThrRS that can non-competitively and tightly bind to ThrRS. The binding site of borrelidin probably represents a new drug target, which will favor the development of aaRS inhibitors. Moreover, it was reported that combining allosteric and ATP-competitive inhibitors can overcome resistance to either agent alone [30]. Therefore, it is necessary to understand the detailed inhibitory mechanism of borrelidin against ThrRS.

Herein, the borrelidin binding site on ThrRS was investigated and the possible inhibitory mechanism of borrelidin against ThrRS was also discussed. The molecular docking demonstrated that borrelidin binds to the region outside but adjacent to the active pocket of ThrRS, which is consisted of residues Y313, R363, R375, P424, E458, G459, and K465 (Fig. 2A). The sequence alignment showed that the residues Y313, P424, E458, and G459 are not conserved in Borrelidin-resistant ThrRSs but varied in Borrelidin-susceptible ThrRSs, which indicated that these four residues may involve the binding of borrelidin and confirmed the possible binding site of borrelidin obtained by molecular docking. Among these four residues, Y313 has been identified as an important residue for borrelidin binding by screening a library of random *E. coli* ThrRS mutants [12]. In order to further validate the important roles of other three residues in borrelidin binding, the mutant P424K, E458Δ, and G459Δ was subsequently constructed by using site-directed mutagenesis, respectively. The results showed that the change of these residues did not affect the enzyme activity but reduced affinity of ThrRS with borrelidin. Therefore, we believed that residues P424, E458, and G459 play important roles in the binding of borrelidin to *E. coli* ThrRS.

Previously, Ruan et al. has proposed that residues L489 and P296 are relevant to borrelidin inhibition, and a hydrophobic region (cluster A) consisting of Thr307, His309, Cys334, Pro335, Leu489 and L493 was predicted as the binding site of borrelidin by *in silico* prediction using the CASTp-pocket/cavity predicting program [12]. However, the relationship between borrelidin inhibition and P296 is still unclear. Due to that P296 belongs to another cavity (cluster C) that far away from cluster A, it is necessary to re-evaluate the binding site of borrelidin. Furthermore, we found that the cluster A is not large enough to accommodate borrelidin when borrelidin was docked to ThrRS. According to the molecular docking results, borrelidin was considered to bind to the region (designated as cluster D) which was outside but adjacent to the active pocket of ThrRS (Fig. 1B). Although cluster A and cluster D only share one amino acid Y313, other amino acids in cluster A with the exception of L493 were observed around cluster D when the residues within 10 Å were selected (Fig. 2B). When the residues within 12 Å were selected, P296 and L493 were then observed. It indicated that cluster A and cluster D may be associated, and structure change of cluster A may induce the structure change of cluster D, which may affect borrelidin binding to cluster D. Thus, it is reasonable to explain why the mutagenesis of any amino acids located in cluster A and cluster D can lead to the change of borrelidin resistance.

Because the docking results may have some deviations, some important residues involving the binding of borrelidin may be missed. Additionally, the residues within 3 Å were selected in this study, which may reduce the number of residues around borrelidin and lead to the loss of some residues non-contacted to borrelidin, such as the residues in cluster A [12]. However, P424, E458, and G459 of *E. coli* ThrRS were identified as the key residues responsible for borrelidin binding by the combination of molecular docking and site-directed mutagenesis analyses. Moreover, the binding site of borrelidin that close to and outside the active site pocket suggested a possible inhibitory mechanism of borrelidin by inducing the cleft closure to avoid release of the products rather than inhibit ATP and threonine binding. In conclusion, the results presented here will contribute to develop novel borrelidin derivatives and accelerate rational design of ThrRS inhibitors.

Acknowledgments

This work was supported in part by grants from the National Outstanding Youth Foundation (No. 31225024), the National Key Project for Basic Research (No. 2010CB126102), the National Key Technology R&D Program (No. 2012BAD19B06), the Program for New Century Excellent Talents in University (NCET-11-0953), the National Natural Science Foundation of China (Nos. 31372006, 31171913 and 31071750), the Outstanding Youth Foundation of Heilongjiang Province (JC201201) and Chang Jiang Scholar Candidates Program for Provincial Universities in Heilongjiang (CSCP).

Appendix A. Supplementary data

Supplementary data associated with this article can be found, in the online version, at http://dx.doi.org/10.1016/j.bbrc.2014.07.100.

References

[1] V. Agarwal, S.K. Nair, Aminoacyl tRNA synthetases as targets for antibiotic development, Med. Chem. Comm. 3 (2012) 887–898.
[2] J.S. Pham, K.L. Dawson, K.E. Jackson, et al., Aminoacyl-tRNA synthetases as drug targets in eukaryotic parasites, Int. J. Parasitol. Drug 4 (2014) 1–13.
[3] P.C. Lv, H.L. Zhu, Aminoacyl-tRNA synthetase inhibitors as potent antibacterials, Curr. Med. Chem. 19 (2012) 3550–3563.
[4] J.E. Rittiner, I. Korboukh, E.A. Hull-Ryde, et al., AMP is an adenosine A1 receptor agonist, J. Biol. Chem. 287 (2012) 5301–5309.
[5] K.R. Mariner, N. Ooi, D. Roebuck, et al., Further characterization of *Bacillus subtilis* antibiotic biosensors and their use for antibacterial mode-of-action studies, Antimicrob. Agents Chemother. 55 (2011) 1784–1786.
[6] D.V.R.N. Bhikshapathi, D.R. Krishna, V. Kishan, Anti-HIV, anti-tubercular and mutagenic activities of borrelidin, Indian J. Biotechnol. 9 (2010) 265–270.
[7] D. Gafiuc, M. Weiss, I. Mylonas, et al., Borrelidin has limited anti-cancer effects in bcl-2 overexpressing breast cancer and leukemia cells and reveals toxicity in non-malignant breast epithelial cells, J. Appl. Toxicol. (2013).
[8] D. Habibi, N. Ogloff, R.B. Jalili, et al., Borrelidin, a small molecule nitrile-containing macrolide inhibitor of threonyl-tRNA synthetase, is a potent inducer of apoptosis in acute lymphoblastic leukemia, Invest. New Drugs 30 (2012) 1361–1370.
[9] I.G. Azcarate, P. Marin-Garcia, N. Camacho, et al., Insights into the preclinical treatment of blood-stage malaria by the antibiotic borrelidin, Br. J. Pharmacol. 169 (2013) 645–658.
[10] T. Nagamitsu, D. Takano, K. Marumoto, et al., Total synthesis of borrelidin, J. Org. Chem. 72 (2007) 2744–2756.
[11] G.H.M. Vondenhoff, A. Van Aerschot, Aminoacyl-tRNA synthetase inhibitors as potential antibiotics, Eur. J. Med. Chem. 46 (2011) 5227–5236.
[12] B. Ruan, M.L. Bovee, M. Sacher, et al., A unique hydrophobic cluster near the active site contributes to differences in borrelidin inhibition among threonyl-tRNA synthetases, J. Biol. Chem. 280 (2005) 571–577.
[13] O. Trott, A.J. Olson, AutoDock Vina: improving the speed and accuracy of docking with a new scoring function, efficient optimization, and multithreading, J. Comput. Chem. 31 (2010) 455–461.
[14] G.M. Morris, R. Huey, W. Lindstrom, et al., AutoDock4 and AutoDockTools4: automated docking with selective receptor flexibility, J. Comput. Chem. 30 (2009) 2785–2791.
[15] Y.M. Gao, X.J. Wang, J. Zhang, et al., Borrelidin, a potent antifungal agent: insight into the antifungal mechanism against *Phytophthora sojae*, J. Agric. Food Chem. 60 (2012) 9874–9881.
[16] J.D. Thompson, D.G. Higgins, T.J. Gibson, CLUSTAL W: improving the sensitivity of progressive multiple sequence alignment through sequence weighting, position-specific gap penalties and weight matrix choice, Nucleic Acids Res. 22 (1994) 4673–4680.
[17] Y. An, J. Ji, W. Wu, et al., A rapid and efficient method for multiple-site mutagenesis with a modified overlap extension PCR, Appl. Microbiol. Biotechnol. 68 (2005) 774–778.
[18] O.H. Lowry, N.J. Rosebrough, A.L. Farr, et al., Protein measurement with the Folin phenol reagent, J. Biol. Chem. 193 (1951) 265–275.
[19] L. Whitmore, B.A. Wallace, Protein secondary structure analyses from circular dichroism spectroscopy: methods and reference databases, Biopolymers 89 (2008) 392–400.

[20] L. Whitmore, B.A. Wallace, DICHROWEB, an online server for protein secondary structure analyses from circular dichroism spectroscopic data, Nucleic Acids Res. 32 (2004) W668–673.
[21] R.A. Copeland, Enzymes: A Practical Introduction to Structure, Mechanism, and Data Analysis, Wiley.com, 2004.
[22] A. Torres-Larios, R. Sankaranarayanan, B. Rees, et al., Conformational movements and cooperativity upon amino acid, ATP and tRNA binding in threonyl-tRNA synthetase, J. Mol. Biol. 331 (2003) 201–211.
[23] E. Seiradake, W. Mao, V. Hernandez, et al., Crystal structures of the human and fungal cytosolic leucyl-tRNA synthetase editing domains: a structural basis for the rational design of antifungal benzoxaboroles, J. Mol. Biol. 390 (2009) 196–207.
[24] Y.K. Zhang, J.J. Plattner, Y.R. Freund, et al., Synthesis and structure-activity relationships of novel benzoxaboroles as a new class of antimalarial agents, Bioorg. Med. Chem. Lett. 21 (2011) 644–651.
[25] D. Ding, Q. Meng, G. Gao, et al., Design, synthesis, and structure-activity relationship of *Trypanosoma brucei* leucyl-tRNA synthetase inhibitors as antitrypanosomal agents, J. Med. Chem. 54 (2011) 1276–1287.
[26] S. Chopra, A. Palencia, C. Virus, et al., Plant tumour biocontrol agent employs a tRNA-dependent mechanism to inhibit leucyl-tRNA synthetase, Nat. Commun. 4 (2013) 1417.
[27] P. Van de Vijver, T. Ostrowski, B. Sproat, et al., Aminoacyl-tRNA synthetase inhibitors as potent and synergistic immunosuppressants, J. Med. Chem. 51 (2008) 3020–3029.
[28] S.F. Ataide, M. Ibba, Small molecules: big players in the evolution of protein synthesis, ACS Chem. Biol. 1 (2006) 285–297.
[29] F.L. Rock, W. Mao, A. Yaremchuk, et al., An antifungal agent inhibits an aminoacyl-tRNA synthetase by trapping tRNA in the editing site, Science 316 (2007) 1759–1761.
[30] J. Zhang, F.J. Adrian, W. Jahnke, et al., Targeting Bcr-Abl by combining allosteric with ATP-binding-site inhibitors, Nature 463 (2010) 501–506.